Cooperative binding of ferrocenylnaphthalene diimide carrying β-cyclodextrin converts double-stranded DNA to a rod-like structure

Shinobu Sato,[†,‡] *Yuta Umeda,*[†] *Satoshi Fujii,*[§] *and Shigeori Takenaka*[†,‡]*

[†]Department of Applied Chemistry, [‡]Research Center for Biomicrosensing Technology, and [§]Department of Bioscience and Bioinformatics, Kyushu Institute of Technology, 1-1 Sensui-cho, Tobata-ku, Kitakyushu, Fukuoka 804-8550, Japan

RECEIVED DATE (to be automatically inserted after your manuscript is accepted if required according to the journal that you are submitting your paper to)

CORRESPONDING AUTHOR FOOTNOTE

Phone: +81-93-884 3322; Fax: +81-93-884 3322; E-mail: shige@che.kyutech.ac.jp.

ABSTRACT

Ferrocenylnaphthalene diimide carrying β-cyclodextrin (β-CD), **1**, intercalated into double-stranded DNA with a binding affinity of $K = (6.6 \pm 0.8) \times 10^4\ M^{-1}$ and a binding site size of n = 4, with a high positive cooperative parameter of ω = 14. β-CD and ferrocene moieties of the compound contributed to the formation of the intermolecular inclusion complex on DNA. Binding of **1** resulted in conversion of the DNA duplex to a rod-like form, which was cleaved upon adamantylamine addition.

KEYWORDS

Naphthalene diimide, ferrocene, β-cyclodextrin, nanowire, double-stranded DNA

INTRODUCTION

β-Cyclodextrin (β-CD) is known to form an inclusion complex with ferrocene, where the reduction and oxidation (Redox) reaction of ferrocene is inhibited by its inclusion, resulting in a positive shift of peak potential with decrease in current.[1, 2] A combination of the electrochemical behavior and molecular recognition ability of β-CD as a host molecule has been utilized in several applications, such as chemical sensors.[2-5] Recently, the formation of such a complex has attracted interest because of its potential application in electrochemical DNA detection. We previously developed a DNA detection system consisting of β-CD and ferrocenylnaphthalene diimide as the DNA ligand,[6,7] with ferrocenyl-β-CD and adamantylnaphthalene diimide[8] or with a naphthalene diimide derivative having β-CD and ferrocene units.[9] Oligonucleotides carrying ferrocene or β-CD at both termini have also been studied with the aim of developing a label-free and signal-on DNA detection system.[10] Oligonucleotides carrying ferrocene or β-CD separately have also been developed in sandwich-type hybridization DNA detection systems, where inclusion complexes are formed in the assembly of two oligonucleotides through target DNA as a template.[11]

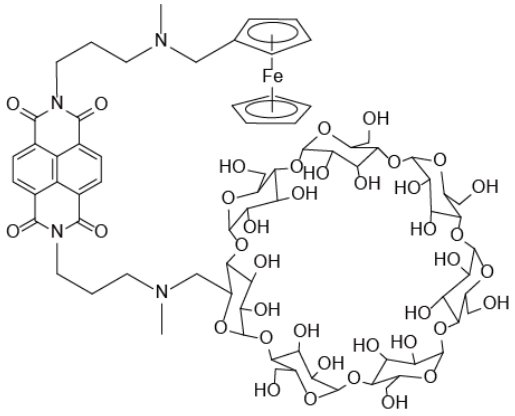

1

Naphthalene diimide derivative is a compound with unique properties and has applications as a semiconductor material, self-assembling nanomaterial forming nanorods or nanotubes, and DNA intercalator.[12-14, 6-9] Ferrocenylnaphthalene diimide carrying β-CD (compound **1**) was designed and synthesized to facilitate the preparation of DNA nanorods. Compound **1** was connected to a naphthalene

diimide with ferrocene and β-CD through a simple linker chain, similar to a previously described compound,[9] but without the triazole moiety from the linker chain. This compound **1** formed an intermolecular complex between ferrocene and the β-CD moiety upon binding to the DNA duplex, converting the DNA duplex into a rod-like form. Recent studies have demonstrated the ability of β-CD inclusion to alter the DNA structure,[10,15-17] providing insights into the regulation of DNA structure by small molecules. Therefore, in this study, we also discuss this topic with respect to our results.

RESULTS AND DISCUSSION

Compound **1** was obtained by the fractionation of its peak using reverse-phase high-performance liquid chromatography (HPLC) after the reaction of N-methyl naphthalene diimide derivatives with trimethylammoniummethyl ferrocene and tosylated β-CD in DMF at 60°C. The cyclic voltammogram of compound **1** in the presence of adamantylamine showed increased peak current with negatively shifted redox potential compared to that in the absence of adamantylamine (Figure S1).

Since β-CD is known to form a more stable inclusion complex with adamantylamine than with ferrocene,[18] this behavior can be explained on the basis of conversion from the intra- or intermolecular inclusion complex of ferrocene with β-CD to a noninclusion complex. AFM measurement of **1** alone did not show any aggregates. Circular dichroism (CD) spectra of **1** alone showed the presence of exciton coupling in the naphthalene diimide chromophore around 300–400 nm, suggesting the stacking of two naphthalene diimide chromophores within the intermolecular inclusion complex of **1** (Figure S2). These results suggested favorable intramolecular complex formation of **1** rather than intermolecular complex formation of **1**.

Thus, compound **1** formed an intramolecular complex in an aqueous solution. Additionally, compound **1** showed an absorption maximum based on the naphthalene diimide chromophore and a hypochromic and red shift upon addition of calf thymus DNA (Figure 1A). Creation of a Scatchard plot using the absorption change upon addition of different amounts of calf thymus DNA yielded a convex upward curve (Figure 1B). A binding constant of $K = (6.6 \pm 0.8) \times 10^4\ M^{-1}$ and binding site size of n = 4,

with a positive cooperative parameter of $\omega = 14$, were obtained by fitting the data to the theoretical equation by McGhee & von Hippel, which considered the cooperative effect.[19] This finding showed that compound **1** bound to the DNA duplex with high positive cooperativity. The binding of compound **1** with double-stranded DNA was clarified by the observations of unwinding of the plasmid DNA in a topoisomerase I assay (Figure S3) and the Cotton effect as an area of induced CD around the region of the naphthalene diimide chromophore in the CD spectrum under excess amounts of calf thymus DNA (Figure S4). Association and SDS-driven dissociation of 2.5 μM compound **1** with 25 μM calf thymus DNA were completed within 45 and 70 s, respectively (Figure S5). The dissociation rate constant of compound **1** from calf thymus DNA was 0.2 s^{-1}, which was one-sixth that of the ferrocenylnaphthalene diimide derivative without β-CD (1.3 s^{-1}), without the intermolecular inclusion complex on DNA[20] (Figure S4B). Similar previously described derivatives[3] have been shown to have a very slow association process over 10 min. The rapid association of compound **1** may be explained by differences in the linker structure without triazole moieties as bulky linkers. According to these results, we propose that compound **1** intercalates double-stranded DNA every four base pairs with very high cooperativity and that this effect may be derived from the formation of an intermolecular inclusion complex between the ferrocene and β-CD moieties of compound **1**.

Figure 2 shows atomic force microscopic (AFM) images of linearized pUC19 DNA (2686 bp) mixed with different amounts of compound **1**. A randomly curving, corded, linear DNA duplex was observed in the case of DNA alone (Figure 2A). In contrast, a rod-like form of the DNA sample was observed when compound **1** was mixed in a 1:1 ratio with DNA (Figure 2D). Such a rod-like structure was not observed for β-CD alone instead (Figure S6). Similar previously described derivatives[3] were also shown to exhibit a rod-like DNA form without repeatability. Compound **1** repeatedly yielded rod-like DNA by reaching a state of equilibrium quickly through rapid association and dissociation. The average DNA lengths were estimated as 398 and 935 nm before and after addition of compound **1**, respectively, by image analysis using Image J software (Figure S7). However, the DNA lengths obtained were not precisely measured because the DNA length observed by AFM is known to be shorter than the

theoretical length when the length is over 50 nm.[21] In our experiment, pUC19 DNA fragments with a theoretical length of 913 nm were observed as strings with an average length of only 398 nm (range, 275–650 nm). The average DNA length after binding to compound **1** increased approximately twofold to 935 nm (range, 650–1400 nm). A previous report also showed that DNA lengths were elongated by 50% and 33% after binding to intercalators with n = 2 or n = 3, respectively.[22] According to the extrapolation of data presented in this paper, the DNA length in the case of n = 4 was expected to be elongated by 25% to approximately 1140 nm. This result seems to be in good agreement with the obtained result.

Figures 2B and C show AFM images in the cases of 1:0.2 and 1:0.5 ratios, respectively, of DNA to compound **1**. Interestingly, rod-like and random coil DNA can be seen together in this AFM image. In particular, for samples with a DNA to compound **1** ratio of 1:0.5, all DNA fragments in the AFM imaging areas showed rod-like structures, and this result was reproducible. This result also showed that compound **1** bound to double-stranded DNA with high positive cooperatively; binding of **1** to double-stranded DNA promoted its binding to the neighboring site of DNA as well. For DNA to compound **1** ratios of over 1:2, DNA aggregates were observed (Figure 2E). This was expected to have resulted from the formation of an intermolecular bridge between DNA strands. In all cases, the DNA complex recovered to the initial random coil structure of DNA upon addition of excess adamantylamine (Figure 2F–I). This may have resulted from the replacement of ferrocene with adamantylamine in β-CD and suggested that formation of the rod-like DNA and DNA aggregates was derived from the β-CD and ferrocene moieties of compound **1**. This finding is also proof that such major structural changes can be attributed to the formation of an inclusion complex between β-CD and ferrocene or adamantylamine. This inclusion behavior was also observed in electrochemical experiments. The cyclic voltammogram of compound **1** was studied in the absence and presence of the linearized pUC19 DNA (Figure 3). Redox peaks based on the inclusion complex of compound **1** with β-CD were observed for the sample with compound **1** alone (Figure 3a), and a decreasing peak current with a slightly negative shift of redox

potential was observed upon addition of DNA (Figure 3b). An increased current peak with a negative shift of the peak was observed upon further addition of adamantylamine to the complex of compound **1** with DNA (Figure 3c). This result also showed that formation of the inclusion complex of ferrocene with β-CD could also be observed, even when the compound was bound to the DNA duplex. Although the peak current of compound **1** alone was larger than that upon addition of adamantylamine to the complex of compound **1** with DNA, the inclusion complex of compound **1** was formed, even when the compound was bound to the DNA. We expected that compound **1** alone formed an intramolecular inclusion complex with its ferrocene and β-CD moieties and that compound **1** was concentrated on the DNA duplex by cooperative intercalation through the inclusion of ferrocene with β-CD, resulting in the rod-like structure shown in Figures 4B and 5. This complex collapsed upon addition of adamantylamine.

Compound **1** bound to double-stranded DNA every 4 base pairs. However, this length did not seem to be sufficient for complex formation between ferrocene and β-cyclodextrin moieties on double-stranded DNA, as shown in Figure 4A. When compound **1** contributed as a cross-linking molecule, as shown in Figure 4B, binding of compound **1** every 4 base pairs and complex formation on double-stranded DNA could be realized. Although spectral changes for **1** upon addition of double-stranded DNA occurred due to the intercalated molecules rather than cross-linking, binding of compound **1** every 4 base pairs was reasonable according to the results of Scatchard analysis. Under the condition of 1:1 ratio of compound **1** and DNA base pair, **1** can bind to DNA duplex every 4 base pairs in light of its binding affinity where excess amount of **1** might contribute cross-linkage between ferrocene and β-CD of **1** on DNA duplex and the linearization seen at a DNA to compound **1** ratio of 1:1 in light of the binding affinity, where the ratio of compound **1** to DNA-bp was 1:2. Figure 5 shows the molecular modeling of the complex containing the intercalated compound **1** bound to the DNA duplex and the crosslinked compound **1**. However, the crosslinked compound **1** did not appear to bind to the groove of the DNA duplex because of the absence of the positive Cotton effect under the naphthalene diimide chromophore (Figure S4). The rod-like structure of the DNA duplex induced by compound **1** was maintained in aqueous solution,

and the random coil structure was observed by high-speed AFM upon addition of adamantylamine (Figure S8, Movie S1).

ACKNOWLEDGMENTS

Our results provided an interesting example of cooperative binding of a small molecule on DNA as a template, and we have discussed the functionalized or fixed structure of DNA in the context of use of DNA as nanomaterials.

This work was supported in part by Grants-in-Aid for Young Scientific Research (B) to S. S. (No. 24750071) from the Ministry of Education, Culture, Sports, Science, and Technology (MEXT).

SUPPORTING INFORMATION PARAGRAPH

The contents of Supporting Information include the following: Theoretical methods and additional results for synthesis of **1**, cyclic voltammogram, topoisomerase I assay, circular dichroism spectra, stopped flow analysis, distribution of DNA length of linearized pUC19 observed AFM, and high-speed AFM (Figures S1–S15).

FIGURE CAPTIONS

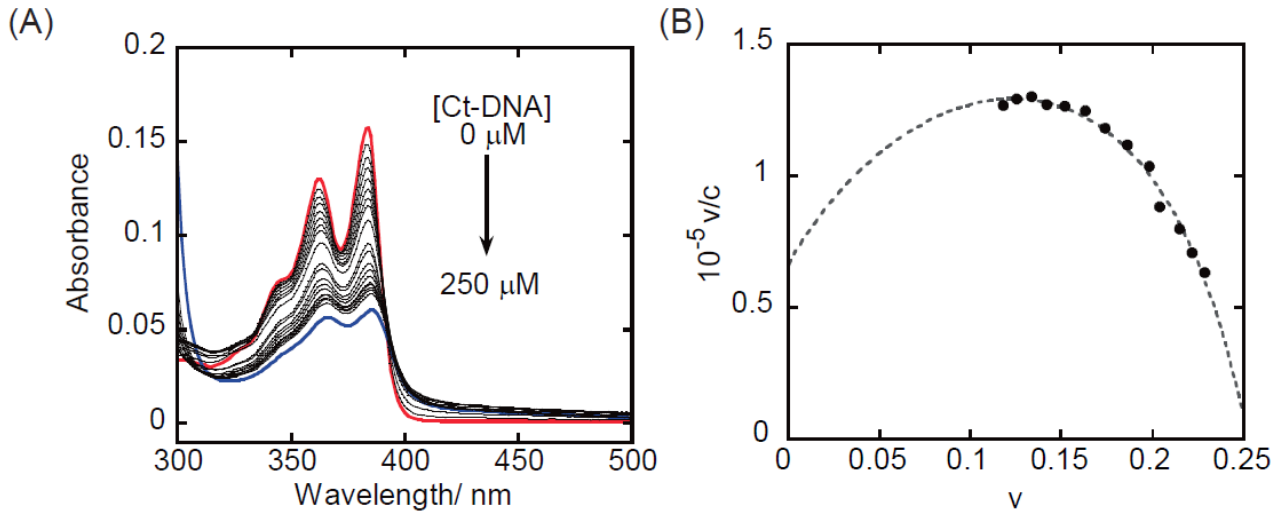

Fig. 1. (A) Absorption change in compound **1** upon addition of calf thymus DNA in 10 mM MES (pH 6.25), 1.0 mM EDTA, and 0.10 M NaCl at 25°C. (B) Scatchard plot based on its spectral change.

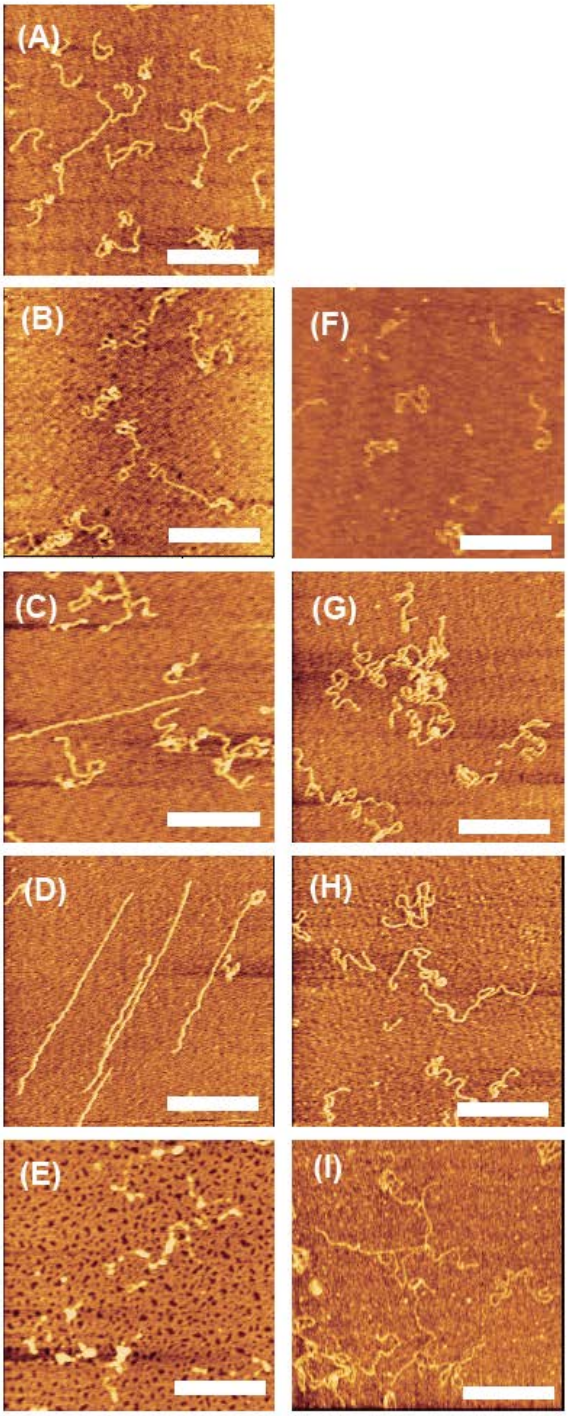

Fig. 2. AFM images of 1.5 μM linearized pUC19 in the absence (A) or presence (B–I) of compound **1**. (B) 1.5 μM pUC19 + 0.30 μM compound **1**, (C) 1.5 μM pUC19 + 0.75 μM compound **1**, (D) 1.5 μM pUC19 + 1.5 μM compound **1**, (E) 1.5 μM pUC19 + 3.0 μM compound **1**, (F) 1.5 μM pUC19 + 0.30 μM compound **1** + 60 μM adamantylamine, (G) 1.5 μM pUC19 + 0.75 μM compound **1** + 150 μM adamantylamine, (H) 1.5 μM pUC19 + 1.5 μM compound **1** + 300 μM adamantylamine, and (I) 1.5 μM

pUC19 + 3.0 μM compound **1** + 60 μM adamantylamine. The white bar scale indicates a length of 500 nm.

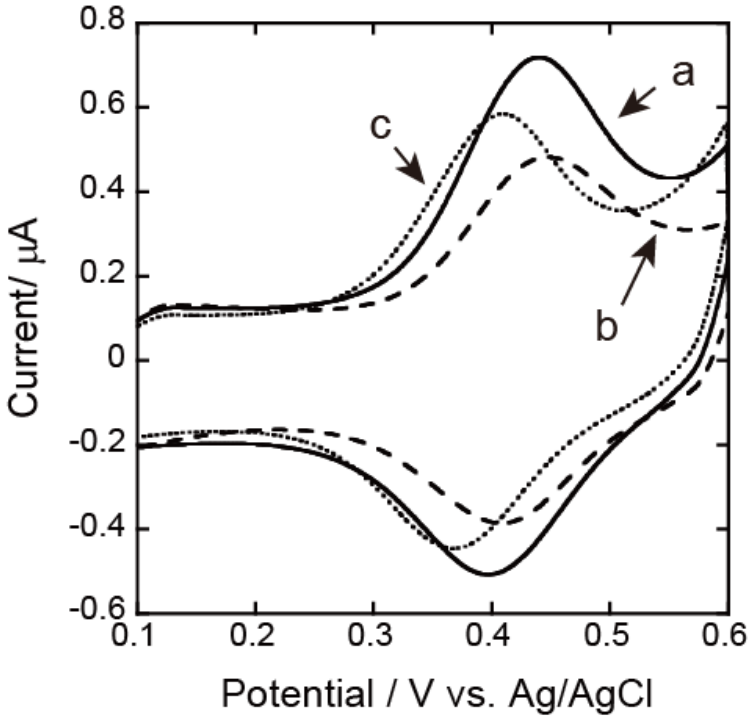

Fig. 3. Cyclic voltammogram of 10 μM compound **1** in the absence (a) or presence of 10 μM linearized pUC19 (b). (c) Cyclic voltammogram **1** in the presence of 10 μM linearized pUC19 and 2.5 mM adamantylamine.

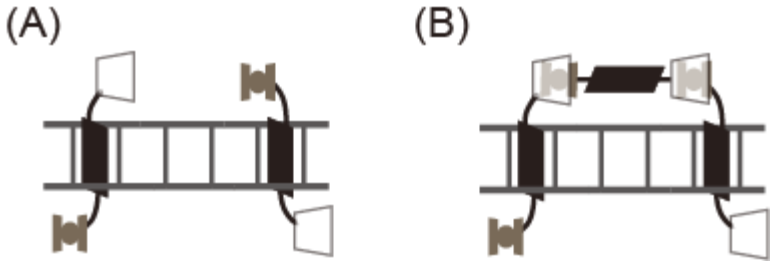

Fig. 4. Schematic illustration of the intermolecular inclusion complex of compound **1** on the DNA duplex.

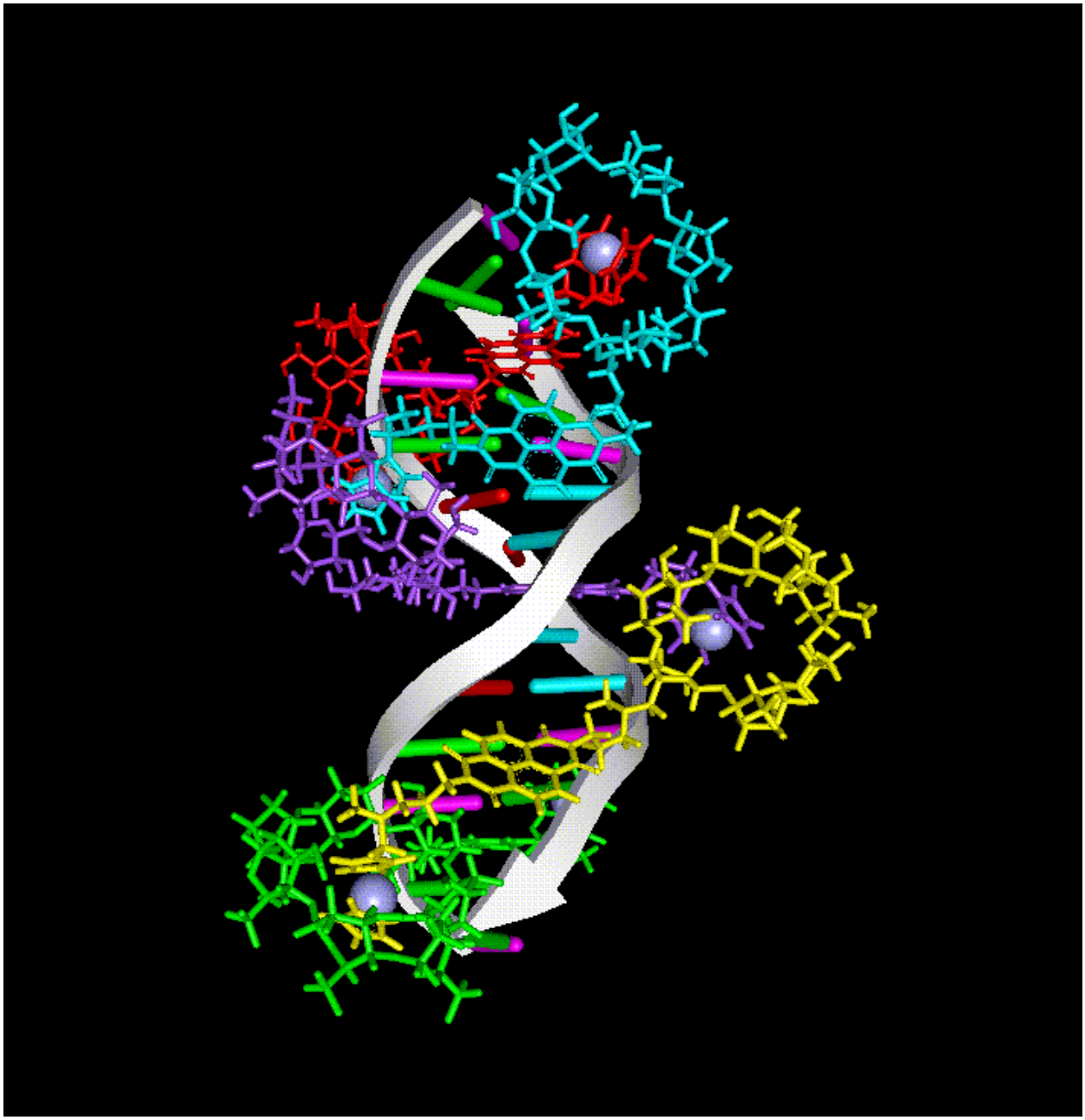

Fig. 5. Molecular modeling of the intermolecular inclusion complex of compound **1** on the DNA duplex.

REFERENCES

1 Lu, D., Ren, X., Liu, L., Zhang, Y., Hu, C., Zhu, H. and Meng, Q. (2002) The inclusion complex of ferrocene with a dithiolene functionalized β-cyclodextrin. *J. Incl. Phenom. Macrocycl. Chem. 43*, 19-23.

2 Martin Del Valle, E. M. (2004) Cyclodextrins and their uses. *Process Biochem. 39*, 1033-1046.

3 Casas-Solvas, J. M., Ortiz-Salmerón, E., Fernández, I., García-Fuentes, L., Santoyo-González, F. and Vargas-Berenguel, A. (2009) Ferrocene–β-cyclodextrin conjugates: synthesis, supramolecular behavior, and use as electrochemical sensors. *Chem. A. Eur. J. 15*, 8146-8162.

4 Chen, M. and Diao, G. M. (2009) Electrochemical study of mono-6-thio-β-cyclodextrin/ferrocene capped on gold nanoparticles: characterization and application to the design of glucose amperometric biosensor. *Talanta 80*, 815-820.

5 Choi, S. J., Choi, G. B. and Park, S. M. (2002) Electrochemical sensor for electrochemically inactive β-d(+)-glucose using α-cyclodextrin template molecules. *Anal. Chem. 74*, 1998-2002.

6 Sato, S., Nojima, T., Waki, M. and Takenaka, S. (2005) Supramolecular complex formation by β-cyclodextrin and ferrocenylnaphthalene diimide-intercalated double stranded DNA and improved electrochemical gene detection. *Molecules 10*, 693-707.

7 Takenaka, H., Sato, S. and Takenaka, S. (2013) Electrochemical detection of duplex DNA using intercalation-triggered decomplexation of ferrocene with β-cyclodextrin. *Electroanalysis 25*, 1827-1830.

8 Sato, S., Nojima, T. and Takenaka, S. (2004) Electrochemical gene detection based on supramolecular complex formation by ferrocenyl-β-cyclodextrin and adamantylnaphthalene diimide bound to double stranded DNA. *J. Organomet. Chem. 689*, 4722-4728.

9 Watanabe, S., Sato, S., Ohtsuka, K. and Takenaka, S. (2011) Electrochemical DNA analysis with a supramolecular assembly of naphthalene diimide, ferrocene, and β-cyclodextrin. *Anal. Chem. 83*, 7290-7296.

10 Ihara, T., Wasano, T., Nakatake, R., Arslan, P., Futamura, A. and Jyo, A. (2011) Electrochemical signal modulation in homogeneous solutions using the formation of an inclusion complex between ferrocene and β-cyclodextrin on a DNA scaffold. *Chem. Commun. 47*, 12388-12390.

11 Aoki, H., Kitajima, A. and Tao, H. (2010) Label-free and 'signal-on' DNA detection using a probe DNA terminated with ferrocene and β-cyclodextrin. *Supramolecular Chem. 22*, 455-460.

12 Bhosale, S. V., Jani, C. H. and Langford, S. J. (2008) Chemistry of naphthalene diimides. *Chem. Soc. Rev. 37*, 331-342.

13 Suraru, S.-L. and Wurthner, F. (2014) Strategies for the synthesis of functional naphthalene diimides. *Angew. Chem. Int. Ed. 14*, 7428-7448.

14 Yen, S. –F., Gabbay, E. J. and Wilson, W. D. (1982) Interaction of aromatic imides with deoxyribonucleic acid. Spectrophotometric and viscometric studies. *Biochemstry 21*, 2070-2076.

15 Cheng, H. B., Zhang, Y. M., Xu, C. and Liu, Y. (2014) Photoresponsive supramolecular complexes as efficient DNA regulator. *Sci. Rep. 4*, 4210.

16 Liu, Y., Yu, Z. L., Zhang, Y. M., Guo, D. S. and Liu, Y. P. (2008) Supramolecular architectures of β-cyclodextrin-modified chitosan and pyrene derivatives mediated by carbon nanotubes and their DNA condensation. *J. Am. Chem. Soc. 130*, 10431-10439.

17 Liu, Y., Yu, L., Chen, Y., Zhao, Y. L. and Yang, H. (2007) Construction and DNA condensation of cyclodextrin-based polypseudorotaxanes with anthryl grafts. *J. Am. Chem. Soc. 129*, 10656-10657.

18 Eftink, M. R., Andy, M. L., Bystrom, K., Perlmutter, H. D. and Kristol, D. S. (1989) Cyclodextrin inclusion complexes: studies of the variation in the size of alicyclic guests. *J. Am. Chem. Soc. 111*, 6765-6772.

19 McGhee, J. D. and von Hippel, P. H. (1974) Theoretical aspects of DNA-protein interactions: co-operative and non-co-operative binding of large ligands to a one-dimensional homogeneous lattice. *J. Mol. Biol. 86*, 469-489.

20 Sato, S. and Takenaka, S. (2008) Linker effect of ferrocenylnaphthalene diimide ligands in the interaction with double stranded DNA. *J. Organomet. Chem. 693*, 1177-1185.

21 Kaji, N., Ueda, M. and Baba, Y. (2001) Direct measurement of conformational changes on DNA molecule intercalating with a fluorescence dye in an electrophoretic buffer solution by means of atomic force microscopy. *Electrophoresis 22*, 3357-3364.

22 Coury, J. E., McFail-Isom, L., Williams, L. D. and Bottomley, L. A. (1996) A novel assay for drug-DNA binding mode, affinity, and exclusion number: scanning force microscopy. *Proc. Natl. Acad. Sci. U. S. A. 93*, 12283-12286.

SYNOPSIS TOC

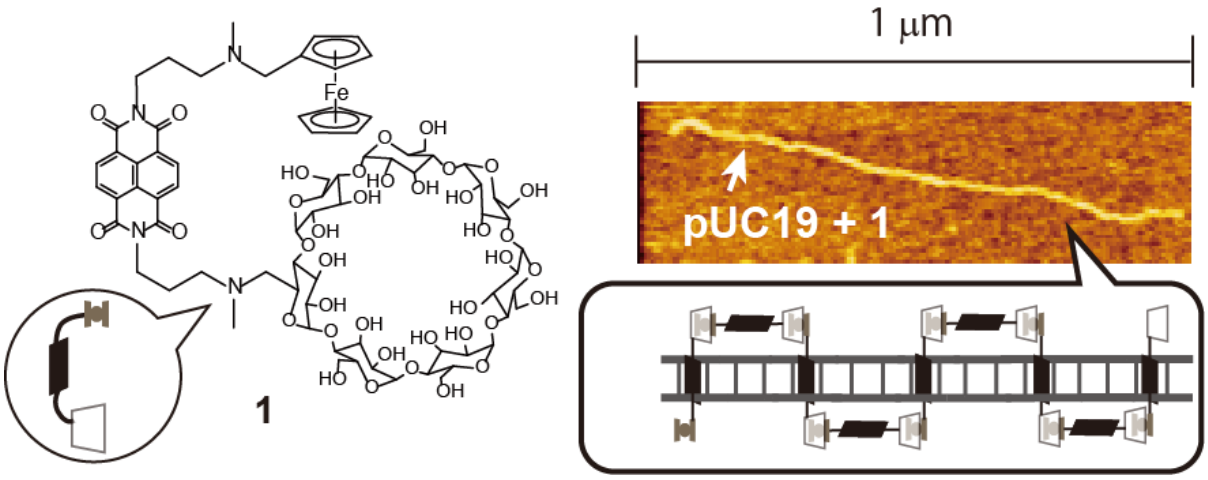

Cooperative binding of ferrocenylnaphthalene diimide carrying β-cyclodextrin converts to a rod-like form of double stranded DNA

Shinobu Sato, [†,‡] Yuta Umeda,[†] Satoshi Fujii,[§] and Shigeori Takenaka[†,‡]*

[†] Department of Applied Chemistry,[‡]Research Center for Biomicrosensing Technology, and [§]Departement of Bioscience and Bioinformatics, Kyushu Institute of Technology, 1-1 Sensui-cho, Tobata-ku, Kitakyushu, Fukuoka, 804-8550, Japan

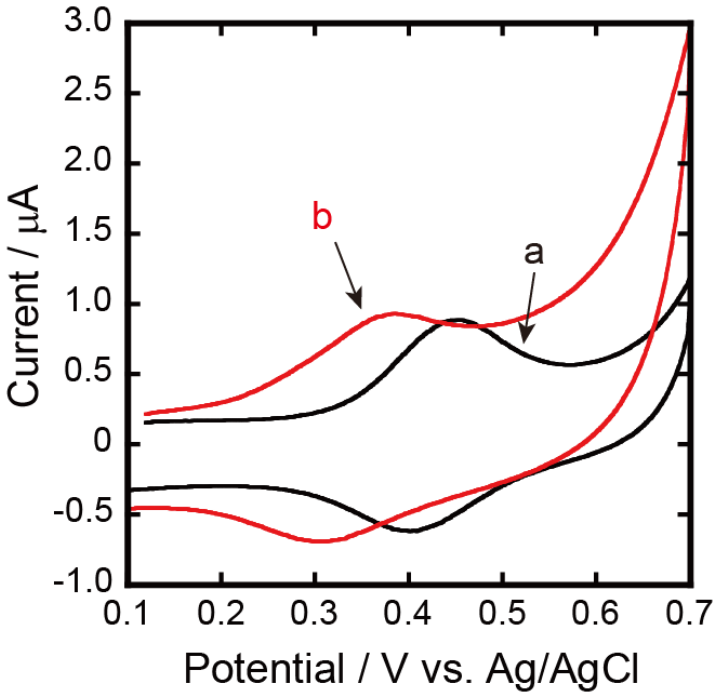

Figure S1. Cyclic voltammograms of GC electrode in 10 mM NaH_2PO_4/Na_2HPO_4 (pH 7.0) containing 100 mM $NaClO_4$ and 10 μM **1** in the absence (a) or presence (b) of 2.5 mM adamantylamine at 25 °C.

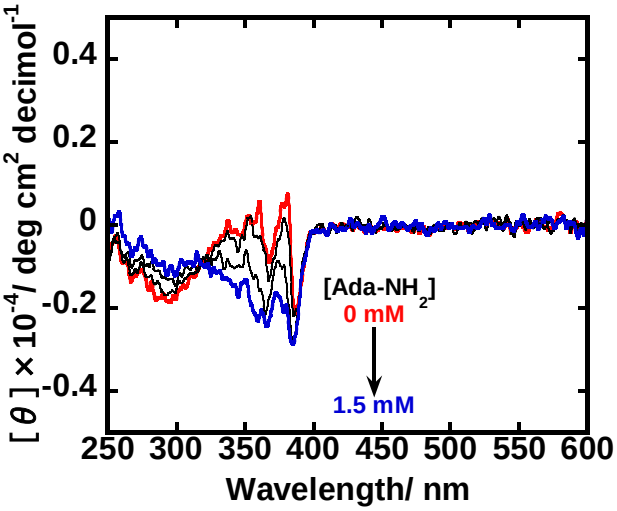

Figure S2. Circular dichromic spectra change at 250-600 nm of 50 μM **1** upon addition of the varied amount of adamantylamine in 10 mM MES buffer and 1.0 mM EDTA (pH 6.25) containing 0.10 M NaCl, 25 °C.

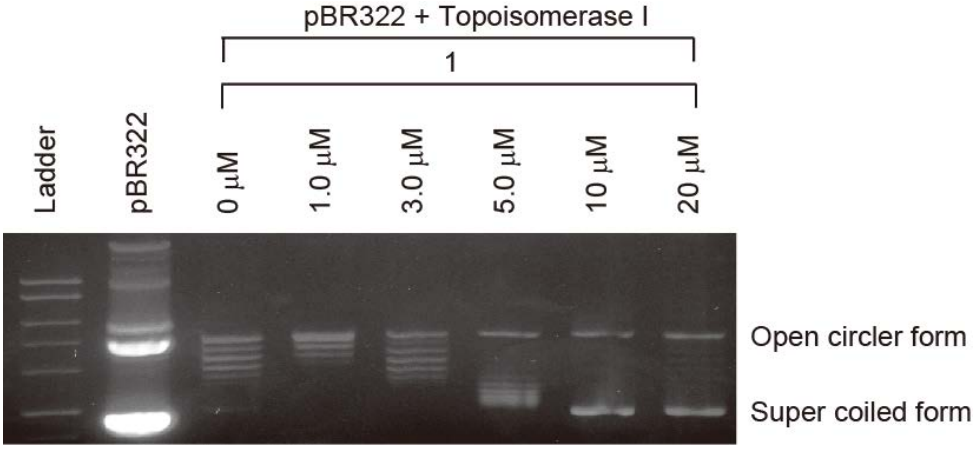

Figure S3. Topoisomerase I assay of **1**. Five unit of Topoisomerase I (Takara bio, Shiga, Japan) was treated with 0.5 μg pBR322 (4361 bp) in 0.01 % BSA and 1×Reaction buffer at 37 °C for 1.0 h in the presence of the varied amount of **1**.

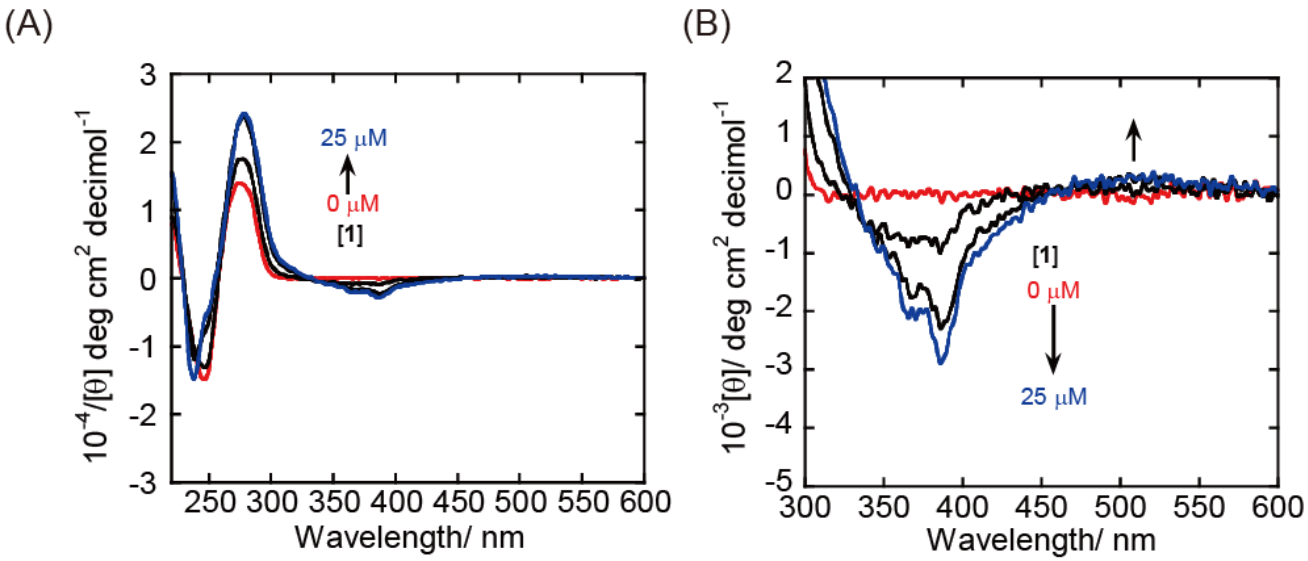

Figure S4. Circular dichromic spectra change at 220-600 nm (A) or 300-600 nm (B) of 70 μM sonicated calf thymus DNA (CT-DNA) upon addition of the varied amount of **1** in 10 mM MES buffer and 1.0 mM EDTA (pH 6.25) containing 0.10 M NaCl, 25 °C.

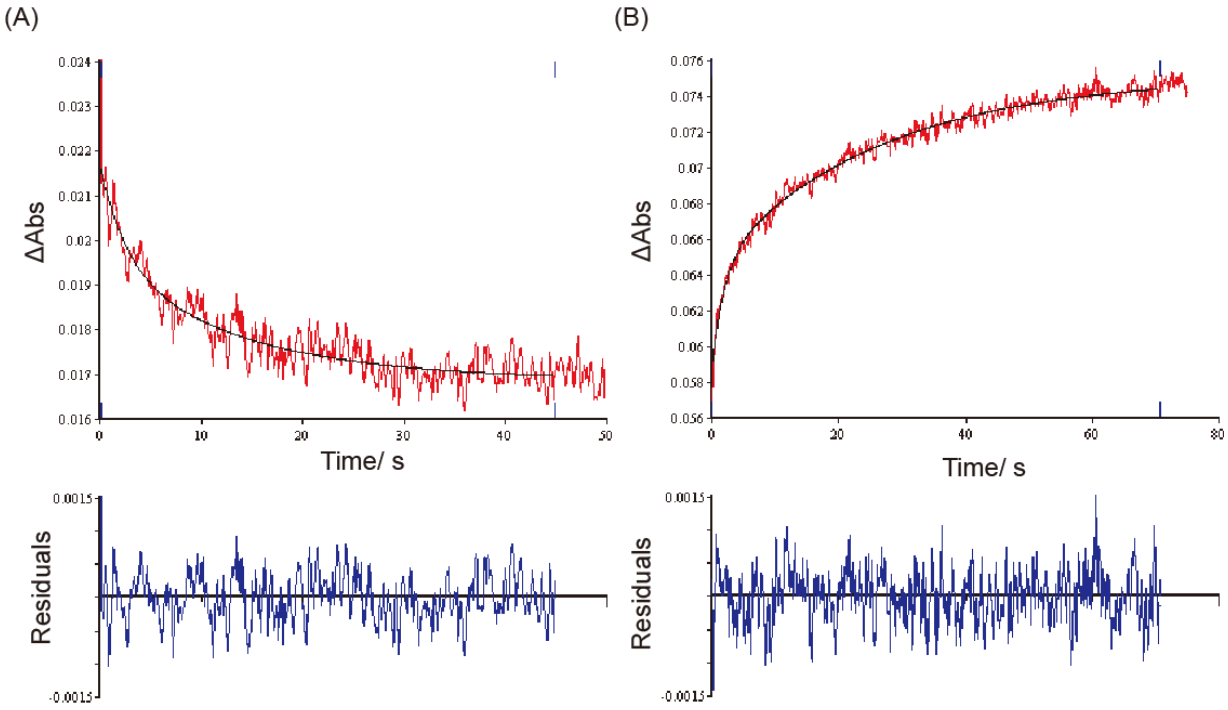

Figure S5. Stopped flow traces for the association (A) and SDS-derived dissociation (B) processes of **1** with CT-DNA in 10 mM MES and 1.0 mM EDTA (pH 6.25) containing 0.1 M NaCl. Absorption changes were measured after mixing with 25 μM-bp CT-DNA and 2.5 μM **1** (A) or after mixing with 0.5% SDS and the solution of 50 μM-bp CT-DNA and 5.0 μM **1** (B).

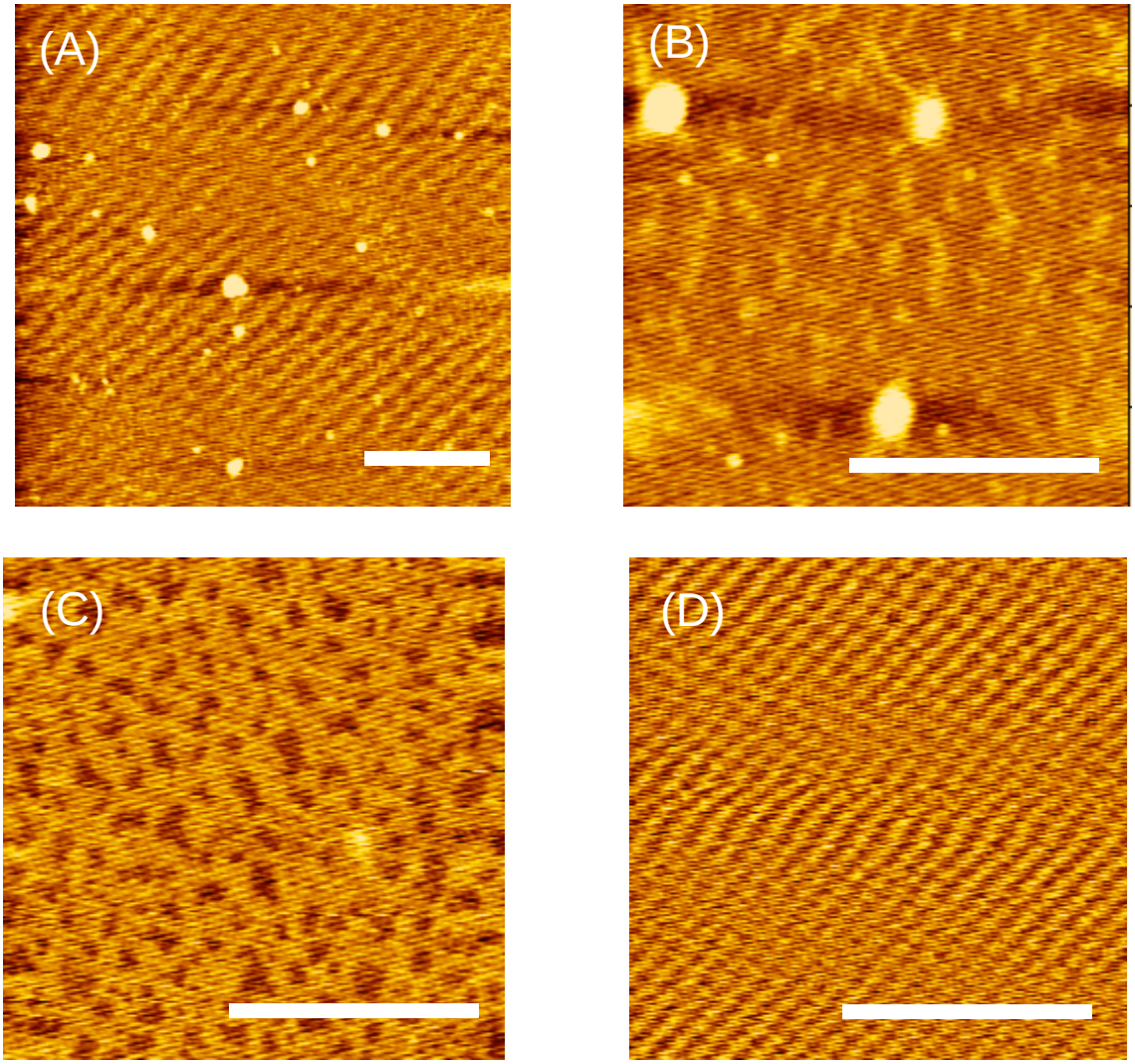

Figure S6. AFM images of 1.5 μM linearized pUC19 + 1.5 μM β-CD (A, B), 1.5 μM pUC19 + 3.0 μM β-CD (C) and 1.5 μM β-CD (D). The white bar scale shows a length of 500 nm.

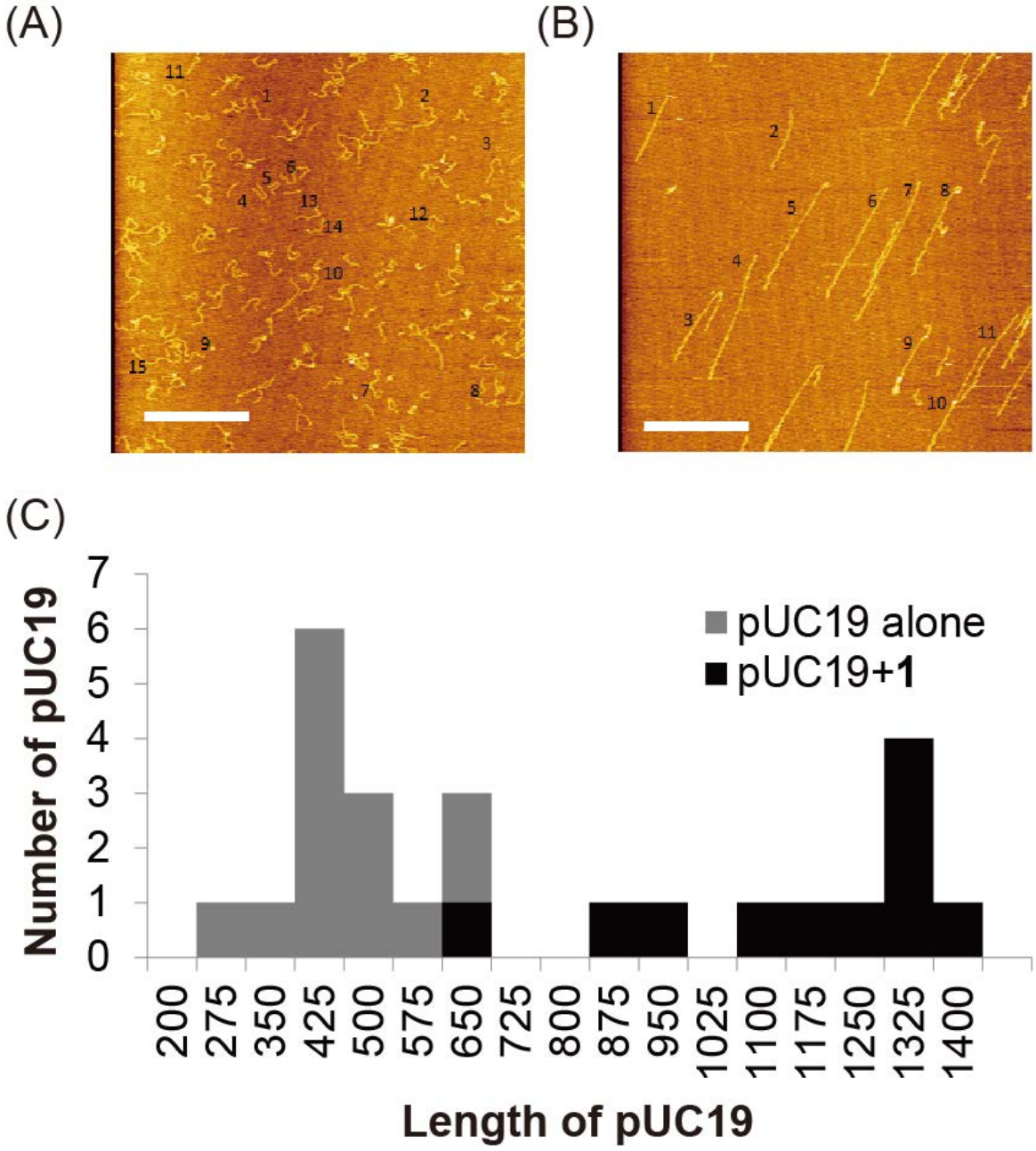

Figure S7. AFM images of 1.5 μM-bp pUC19 in the absence (A) or presence of 1.5 μM **1** (B). (C) Histogram of pUC19 length obtained from their images in the absence (A, gray bar) or presence of **1** (B, black bar). The white bar scale shows a length of 1000 nm.

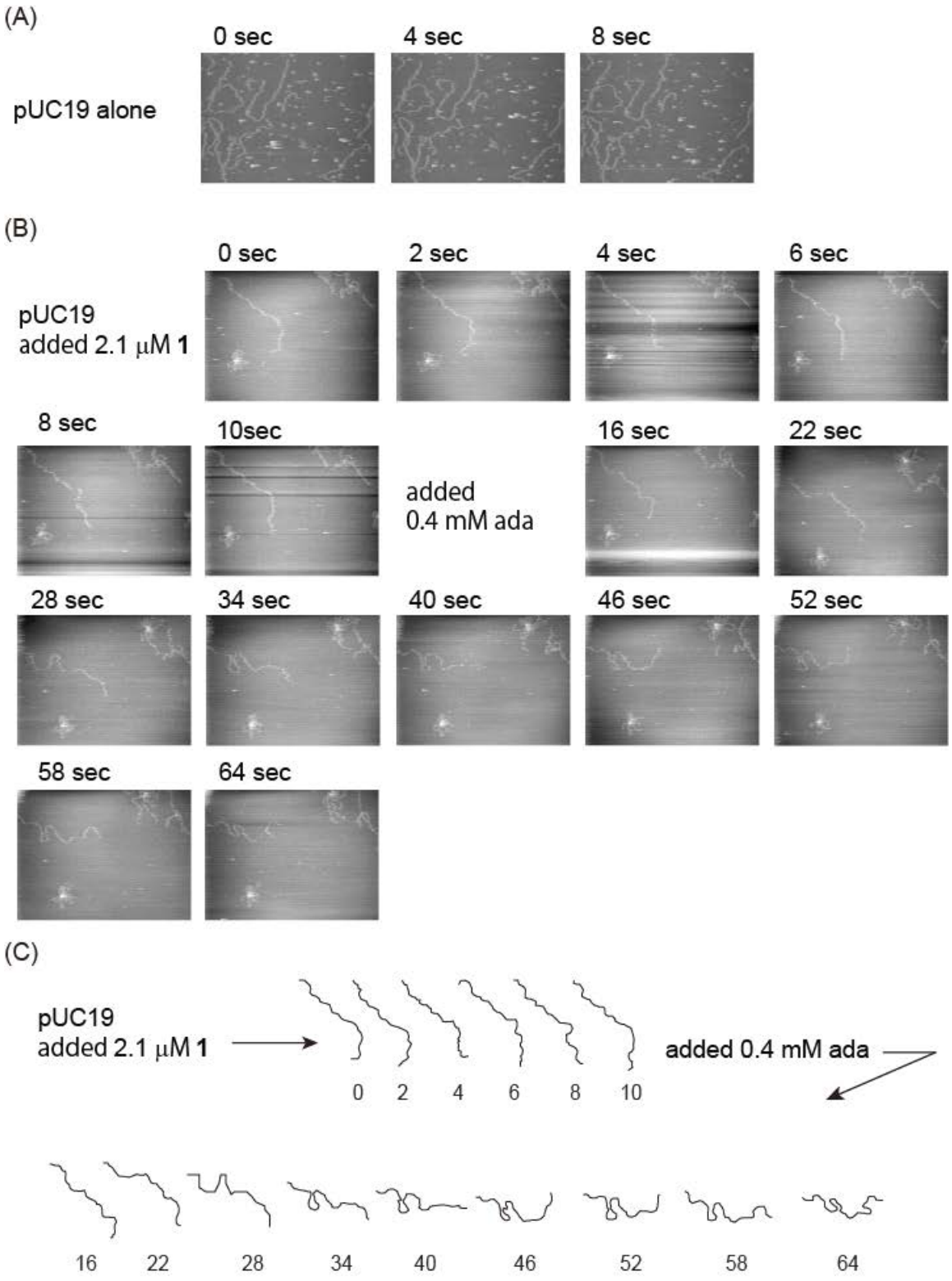

Figure S8. High Speed AFM images of the combination of linear pUC19, **1**, and/or Ada-NH_2: (A) 0.6 μM-bp linear pUC19 in a Milli Q water containing 10 mM $MgCl_2$, (B) 0.6 μM-bp linear pUC19 in 5 mM $MgCl_2$ after addition of 2.1 μM **1** at 0 s and subsequently imaging further addition of 0.4 mM Ada (after 16 s). Imaging area; 750×1000 nm, imaging rate; 0.5 fps. (C) DNA shape traces of (B) depending on the time.

Experimental Section

Synthesis of ferrocenylnaphthalene diimide 1

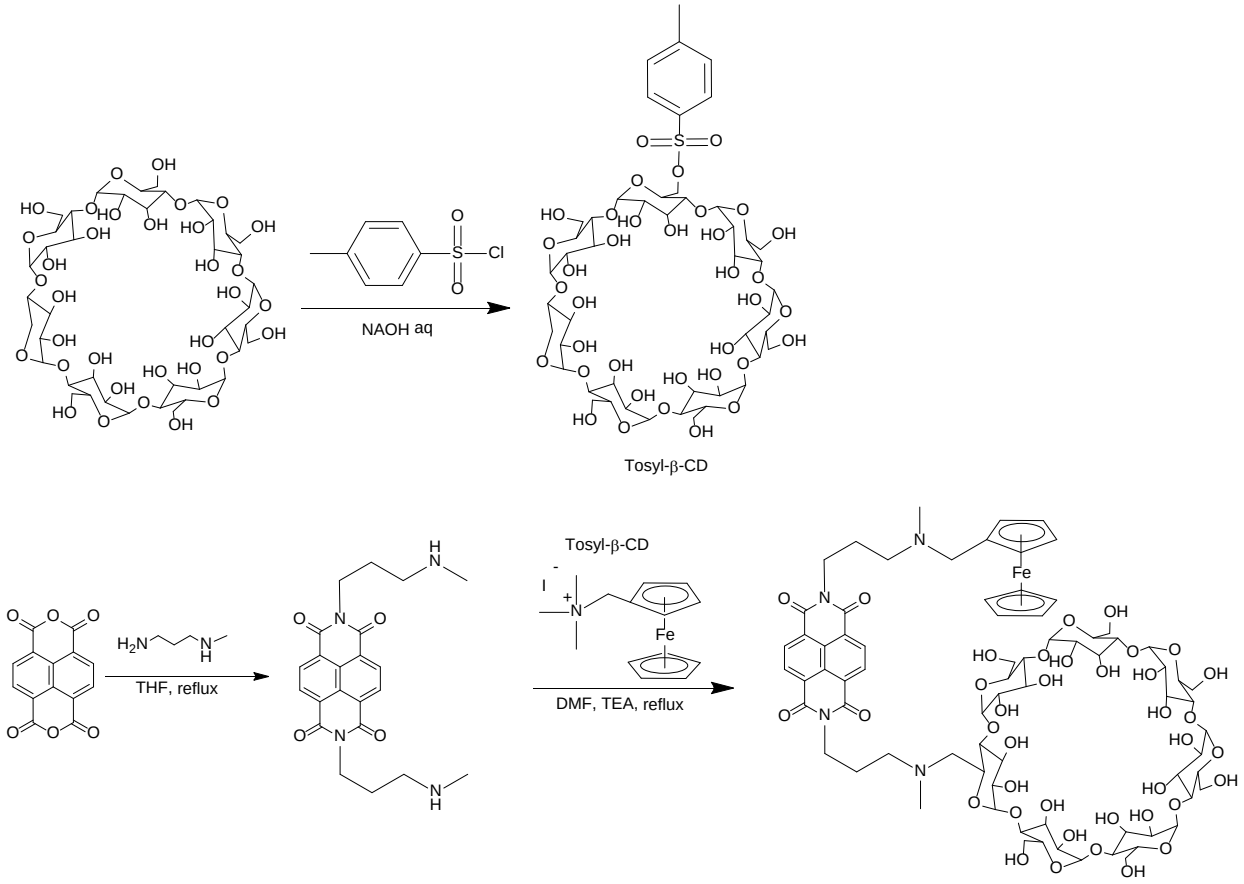

N,N'-Bis(3-methylaminopropyl)naphthalene-1,4,5,8-tetracarboxylic acid diimide[1] and Tosyl-β-CD[2] were synthesized by the route previously reported. Tosyl-β-CD; ^{1}H-NMR (500 MHz, DMSO-d_6): δ= 2.59 (3.22/3H, s), 3.20-3.80 (148.29/42H, bm), 4.15-4.60 (6.56/6H, bm), 4.75-4.90 (7.29/7H, m), 5.60-5.95 (14.23/14H, bm), 7.43 (2.02/2H, d, J=8.0 Hz), 7.75 (2.00/2H, d, J=8.3 Hz) ppm.

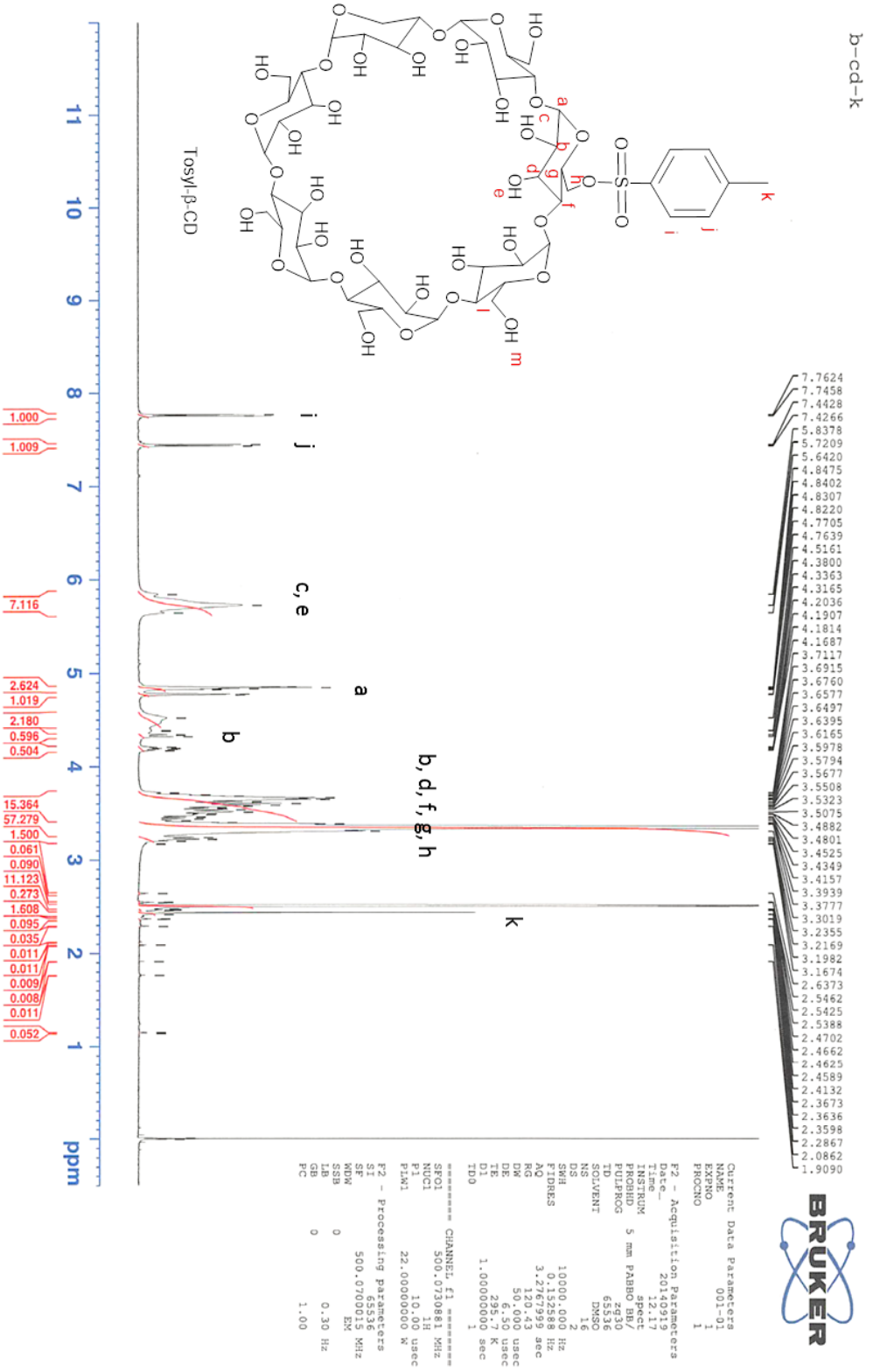

Figure S9. ^{1}H-NMR chart of 6-O-Monotosyl-6-deoxy-β-cyclodextrin in DMSO-d_6 using TMS as internal standard.

A solution of (ferrocenylmethyl)trimethylammonium iodide (0.14 g, 0.35 mmol), N, N'-Bis(3-methylaminopropyl)naphthalene-1,4,5,8-tetracarboxylic acid diimide 0.14g, 0.35 mmol), and Tosyl-β-CD (0.46 g, 0.35 mmol) in DMF (10 ml) was stirred at 60 °C for 190 h and DMF was removed under reduced pressure. The residue was dissolved in 0.1 % TFA and applied to the reversed phase high performance liquid chromatography (HPLC) on Inertsil ODS-3 (inner diameter 5 mm, size 4.6 x 250 mm, GL Science Inc., Japan) in a gradient mode at a flow rate of 1.0 ml/min, where the concentration of acetonitrile was changed linearly to 38.5 % from 7.0 % in water containing 0.1% trifluoroacetic acid over 30 min. Elution was monitored by absorption at 250-400 nm (Figure S6). The peak at 23 min of retention time was collected as target **1**. Lyophilization of the collected eluents gave 0.041 g (0.024 mmol, 6.7% yield) of **1** as a white powder. MALDI-TOF-MS (positive mode, α- CHCA) m/z=1724.62 (Theory for $C_{75}H_{102}N_4O_{38}Fe+H^+$ = 1724.44). ^{1}H-NMR (500 MHz, DMSO-d_6): δ= 2.10 (4.32/4H, bm), 2.50 (3.89/3H, s), 2.51 (3.12/3H, s) 2.91 (1.00/2H, d), 3.00 (1.76/2H, bm), 3.1-3.90 (88.44/34H, bm), 4.0-4.4 (19.52/19H), 4.75-5.00 (8.54/7H, bm), 5.50-6.15 (13.68/14H, m), 8.71, and 8.72 (4.00/4H, s and s) ppm. ^{13}C-NMR (500 MHz, DMSO-d_6): δ=22.98, 38.88, 52.41, 55.41, 60.18, 61.51, 69.33, 69.42, 70.51, 71.49, 72.42, 72.61, 72.79, 73.26, 73.35, 75.02, 80.51, 81.35, 82.03, 84.46, 101.09, 102.39, 126.82, 131.00, 158.28, and 163.17 ppm. HRMS Calcd. for C38H50N6O6+H$^+$: M, 1723.5589. Found: m/z 1723.5581.

1) Sato, S.; Nojima, T.; Waki, M.; Takenaka, S. *Molecules* **2005**, 10, 693-707.

2) Matsue, T.; Evans, D. H.; Osa, T.; Kobayashi, N. *J. Am. Chem. Soc.* **1985**, 107, 3411-3417.

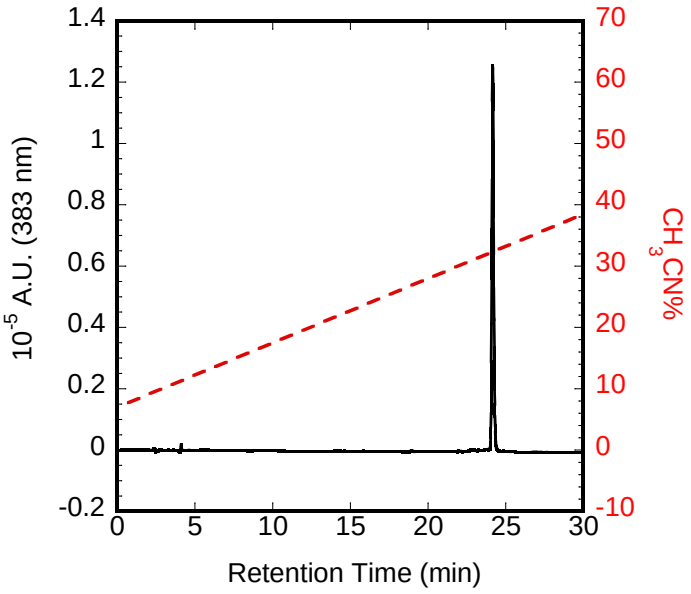

Figure S10. Reversed phase HPLC chart of **1**. The concentration of acetonitrile was changed linearly to 38.5% from 7.0% in water containing 0.1% trifluoroacetic acid over 30 min at 40 ˚C.

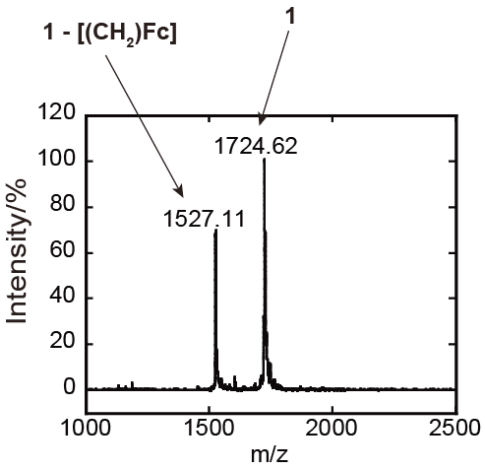

Figure S11. MALDI-TOF-MS spectra of **1** (positive mode, α- CHCA)**.**

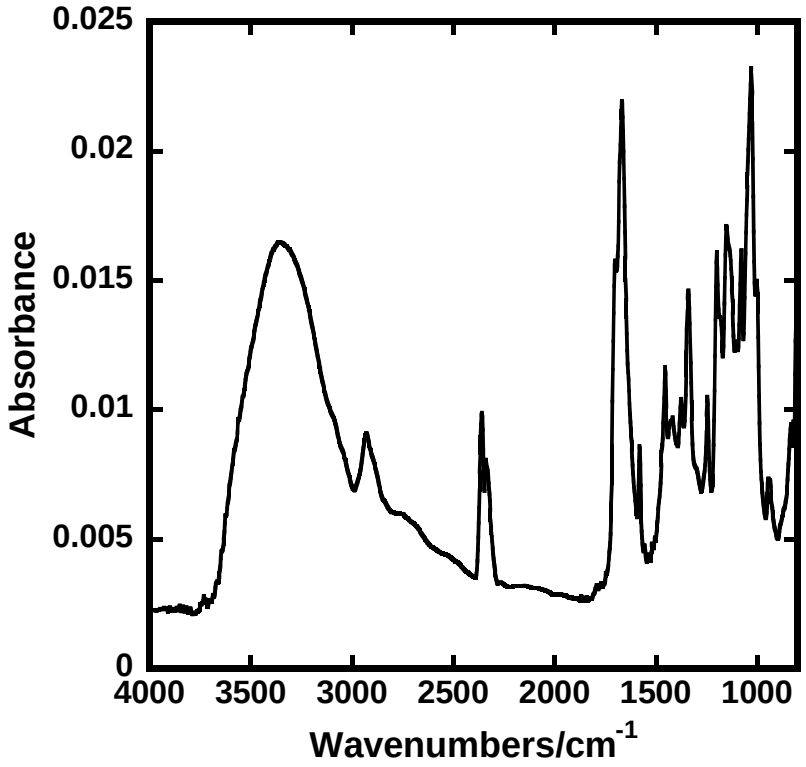

Figure S12. Fourier transform infrared (FT-IR) spectroscopy chart of compound**1**.

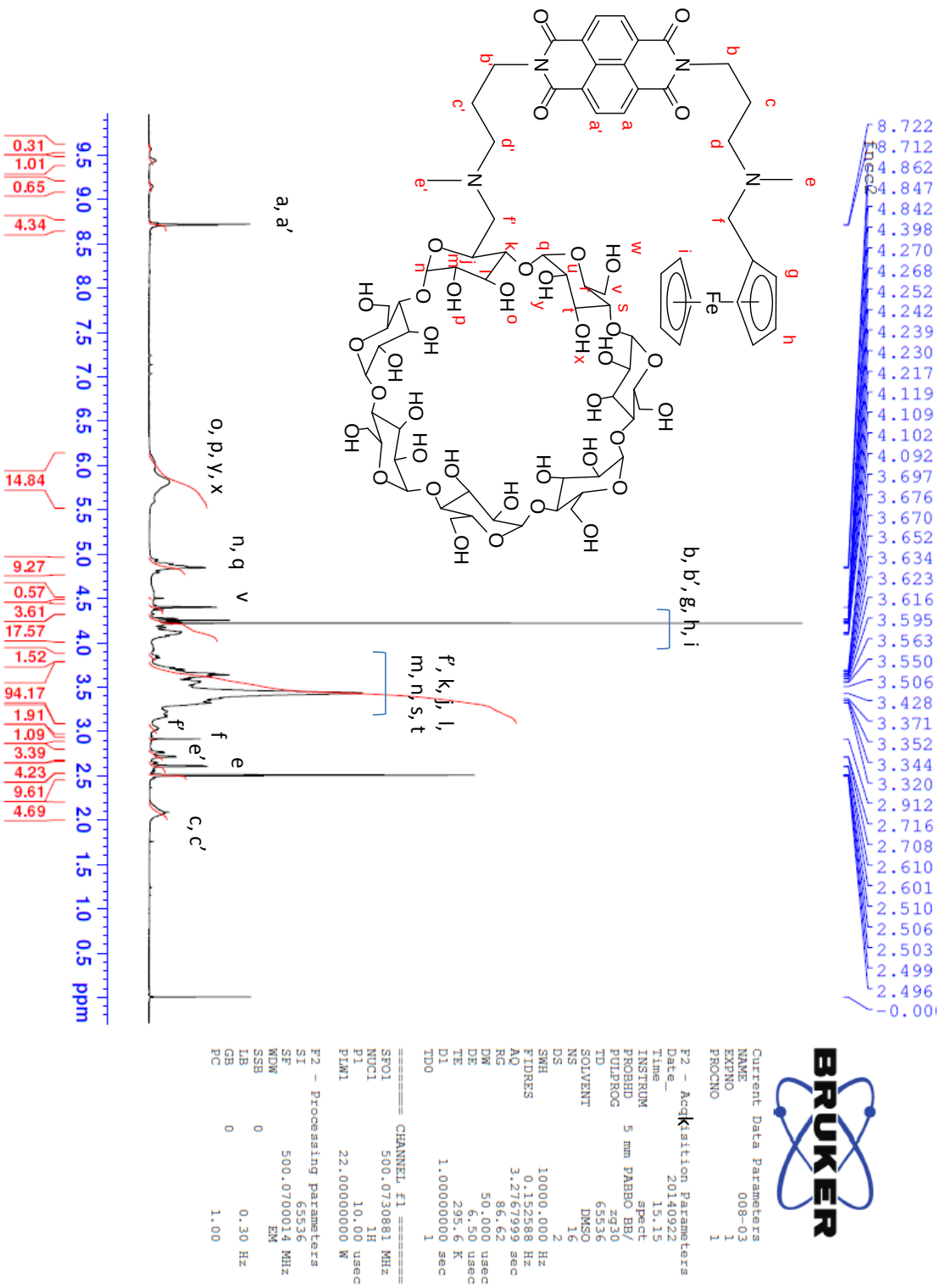

Figure S13. ^{1}H-NMR chart of compound **1** in DMSO-d_6 using TMS as internal standard.

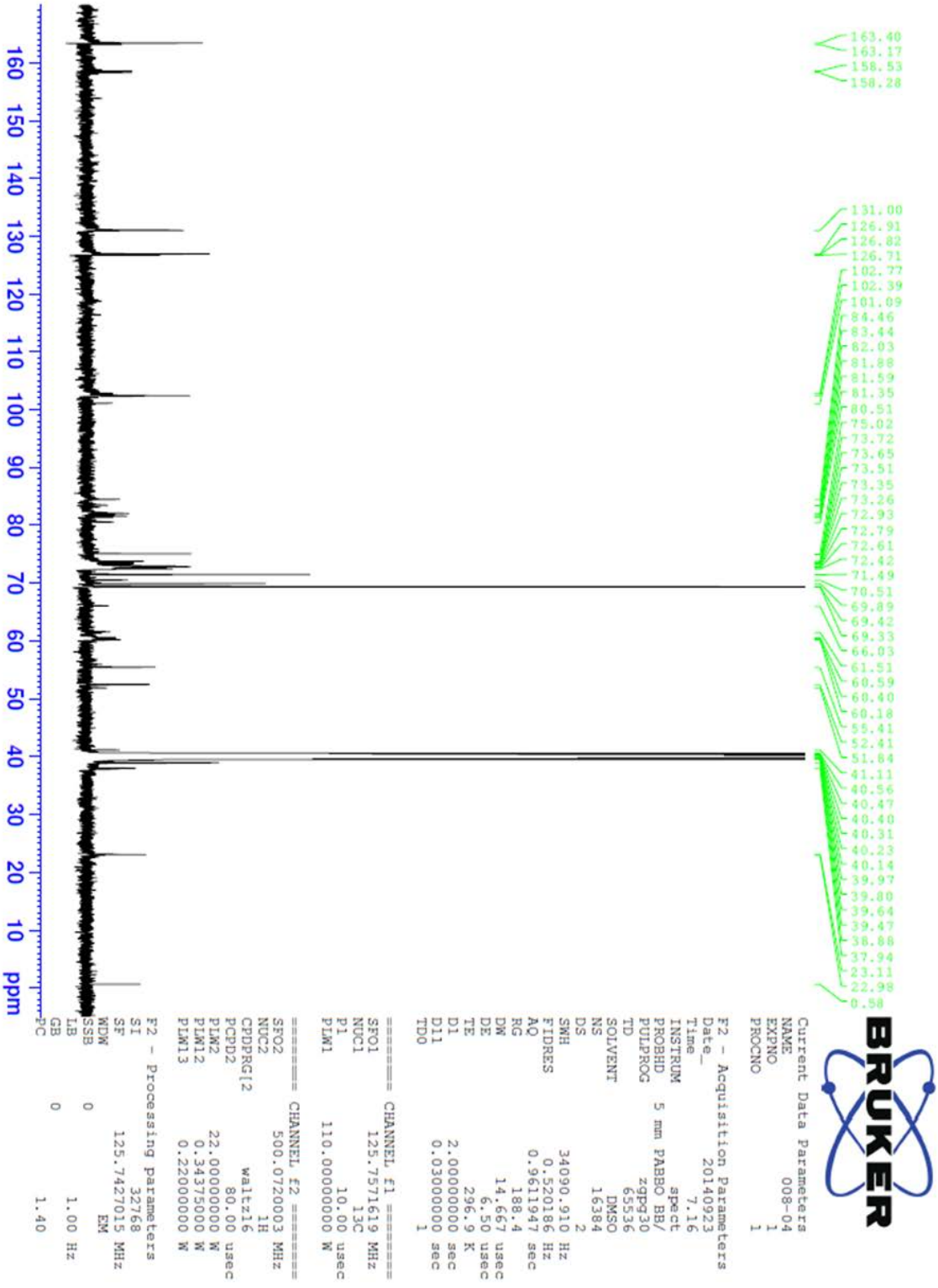

Figure S14. ^{13}C-NMR chart of compound**1** in DMSO-d_6 using TMS as internal standard.

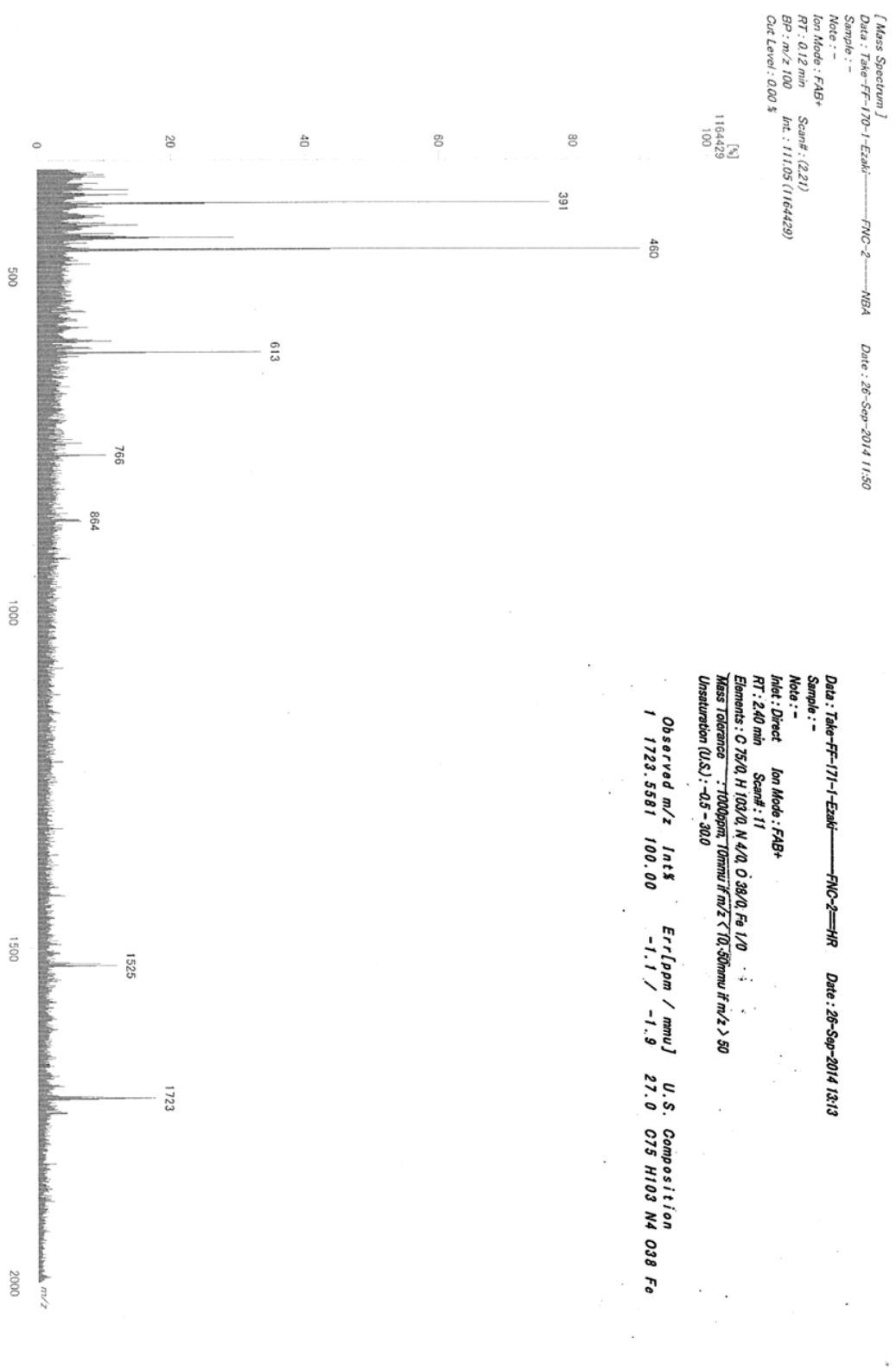

Figure S15. High-resolution mass spectra (HRMS-FAB) of compound **1.**

Apperaus

FT-IR spectra were measured by ALPHA FT-IR Spectrometer (Bruker Optics). The mass spectra (MS) were recorded using a Voyager^{TM} Linear-SA (PerSeptive Biosystems, Foster City, CA) by the time-of-flight mode with α-cyano-4-hydroxycinnamic acid as the matrix.

Sample preparation

The lyophilizate of **1** was added 1.5 mL of Milli-Q and the solution was measured by Hitachi U-3310 spectrophotometer (Tokyo, Japan) at 25 °C. The concentration of **1** was calculated by using molar absorbance coefficient; 27000 cm^{-1} M^{-1} at 383 nm.

Cyclic voltammetry measurement of 1 in the absence of presence of adamantylamine

A GC electrode was polished by 0.05 μm of alumina slurry. Cyclic voltammetry (CV) measurements were performed at 25 °C with a three-electrode configuration consisting of an Ag/AgCl reference electrode, a Pt counter electrode, and a pretreatment GC electrode as the working electrode. Ten μM of **1** in 10 mM NaH_2PO_4/Na_2HPO_4 (pH 7.0) containing 100 mM $NaClO_4$ was measured in the absence of presence of 2.5 mM adamantylamine by ALS650C (CH Instrument, Austin, TX). The following parameters were employed: CV, scan range = 0.1 - 0.7 V, scan rate = 0.1 V/s, sweep segments = 2, sample period = 0.001 V, quiet time = 2.0 s, sensitivity = 1 x 10^{-6} A/V.

Circular dichroism (CD) spectral measurements

Various concentrations of adamantylamine were added to 50 μM **1** in 10 mM MES buffer and 1.0 mM EDTA (pH 6.25) containing 0.10 M NaCl, 25 °C and CD spectra taken at a scan rate 50 nm/min on a Jasco J-820 spectropolarimeter (Tokyo, Japan).

Various concentrations of **1** were added to 70 μM CT-DNA in 10 mM MES buffer and 1.0 mM EDTA (pH 6.25) containing 0.10 M NaCl, 25 °C and CD spectra taken at a scan rate 50 nm/min on a Jasco J-820 spectropolarimeter (Tokyo, Japan). Further CD conditions were as follows: response 2.0 s, data interval 0.10 nm, sensitivity 100 mdeg, bandwidth 2.0 mm, and scan number 4 times.

Topoisomerase I assay

Topoisomerase I assay was carried out according to a procedure described previously.[3]

3) Esaki, Y.; Islam, Md. M.; Fujii, S.; Sato, S.; Takenaka, S. *Chem. Commun*. **2014**, 50, 5967-5969.

Scatchard analysis

The binding affinity of **1** for sonicated calf thymus DNA (CT-DNA) as a dsDNA was determined by a Hitachi U-3310 spectrophotometer equipped with an SPR 10 temperature controller under the following conditions: 25 °C; slit width, 5 nm; speed, 600 nm min^{-1}. Absorption change of 5.0 μM of **1** monitored at 384 nm upon addition of CT-DNA in 10 mM 2-(N-morpholino)ethanesulfonic acid (MES) (pH 6.25), 1.0 mM ethylenediaminetetraacetic acid (EDTA), and 0.10 M NaCl. Scatchard analysis using the condition probability method of McGhee and von Hippel shown as follows: $v/c=K(1-nv)\{[(2\omega-1)(1-nv)+(n-R)]/[2(\omega-1)(1-nv)]\}^{n-1}\{[1-(n-1)v+R]/[2(1-nv)]\}^2$, where *v*, *c*, *K*, R, ω, or *n* refers to the moles of **1** bound per DNA base pair, the free **1** concentration, the observed binding constant, $R=\{[1-(n+1)v]+4\omega n(1-nv)\})^{1/2}$, cooperative parameter or site size as the number of base pairs excluded by drug molecules, respectively.

Stopped flow analysis

Kinetic experiments were performed with an SF-61 DX2 double mixing stopped flow system (Hi-Tech Scientific Inc., UK) equipped with a temperature controller Lauda RE206. Single wavelength kinetic records of absorbance versus time were collected by mixing with 50 μM CT-DNA and 5.0 μM in 10 mM MES, buffer (pH 6.2) 1.0 mM EDTA, and 0.10 M NaCl. Absorbance was collected at 383 nm, the wavelength where absorption of **1** is maximum.

The dissociation rate constant (k_d) of **1** from CT-DNA was determined by the sodium dodecylsulfate (SDS)-dissociation measurement established by the previous papers. Two kinds of reaction solutions (1.0% SDS and 100 μM CT-DNA - 10 μM **1** complex) were mixed instantaneously using a piston, and the change in the absorption spectrum was measured soon after mixing. Thus, when the CT-DNA-**1** complex was mixed with an SDS solution, free **1** was incorporated into the SDS micelle. Since this process is diffusion-controlled, the entire absorption change represents the k_d-dependent process and, therefore, the fitting of kinetic trace provided k_d values.

AFM measurement

AFM measurement was carried out according to a procedure described previously.[3]

The mica surface was exfoliated with adhesive tape, 40 μl of 10 ppm poly-L-lysine placed on it, allowed to stand for 5 min, washed twice with Milli-Q water (100 μl), and dried with an N_2 gas for 30 min. Samples (see Table S1) in 10 mM Tris-HCl (pH 8.0) and 1.0 mM EDTA were placed on the mica surface prepared be the above procedure and washed twice with Milli-Q water (100 μl), dried overnight in a desiccator, and finally with an N_2 gas for 30 min. AFM images were taken on an Nanonavi IIs station and nanocute in the dynamic force mode with a cantilever (PRC-DF40P, SII Nanotechnology, Tokyo, Japan).

Table S1. Sample information

Sample in Fig. 2	1 /μM	$AdaNH_2$ /μM	Linearized pUC19* /μM-bp
A	0	0	1.5
B	0.30	0	1.5
C	0.75	0	1.5
D	1.5	0	1.5
E	3.0	0	1.5
F	0.30	60	1.5
G	0.75	150	1.5
H	1.5	300	1.5
I	3.0	60	1.5

* linearized pUC19 DNA was prepared from the digestion with EcoRI

High speed AFM measurement

Mica surface was exfoliated with adhesive tape, 2.0 μl water containing 0.6 μM-bp pUC19, 2.1 μM **1**, and 5 mM $MgCl_2$ were placed on it and allowed to stand for 5 min. It was washed twice with 10 mM $MgCl_2$ (20 μl). The mica was placed on an Nano Live Vision (Research Institute of Biomolecule Metrology Co., Ltd., Tsukuba, Japan) with 120 μL of 10 mM $MgCl_2$ as measurement solution. AFM images were taken with a cantilever (BL-AC10EGS-A2, Research Institute of Biomolecule Metrology Co., Ltd.) by 0.5 fps. After monitoring 1-pUC19 complex, 5 μL of 10 mM adamantylamine was added to measurement solution. Image range; 825 nm × 1100 nm

Cyclic voltammetry measurement of 1-DNA in the absence of presence of adamantylamine

A GC electrode was polished by 0.05 μm of alumina slurry. Cyclic voltammetry (CV) measurements were performed at 25 °C with a three-electrode configuration consisting of an Ag/AgCl reference electrode, a Pt counter electrode, and a pretreatment GC electrode as the working electrode. The mixture of 10 μM **1** and 10 μM-bp linearized pUC19 in 10 mM NaH_2PO_4/Na_2HPO_4 (pH 7.0) containing 100 mM $NaClO_4$ was measured in the absence of presence of 2.5 mM adamantylamine with ALS650C (CH Instrument, Austin, TX). Employed parameters were as follows: scan range = 0.1 - 0.7 V, scan rate = 0.1 V/s, sweep segments = 2, sample period = 0.001 V, quiet time = 2.0 s, and sensitivity = 1×10^{-6} A/V.

Computer modeling of the complex of double stranded 15-meric double stranded oligonucleotide with 1

Molecular modeling of the complex was calculated with MOE[4] using MMFF94x force field. Force field of ferrocene was used with the adjustment of geometry and formal charge with the distance constraint between iron and carbon to keep its structure during molecular computation by MOE after its structural optimization by PM6 of MOPAC2009. Double stranded 15-meric oligonucleotide of d(GCG CGC GCG CGC GCG C)$_2$ was constructed by Create Sequence of MOE as B-helix. Five binding sites were created and calculated to minimalize their over disorders energetically during short period and compound **1** is inserted these binding sites and calculated with the distance constraint to interact between β-cyclodextrin and ferrocene moieties of **1** under the fixed structure of DNA. After obtained the inclusion structure between β-cyclodextrin and ferrocene moieties of **1** on DNA duplex, its mineralization was carried out without any distance constraint. Several obtained structures with energetically-low level were picked up and further mineralization of these structures was carried out and the obtained the lowest level of the structure was shown in Fig. 4.

4) Molecular Operating Environment (MOE).2011.10., Chemical Computing Group (CCG) http://www.chemcomp.com/